JOURNAL OF MATERIALS SCIENCE 7 (1972) 621–626

# The Effect of Firing Temperature on Properties of Natural Steatite and Pyrophyllite*

JOE B. KERSEY†, R. CRAIG JERNER
*School of Chemical Engineering and Materials Science, University of Oklahoma, Norman, Oklahoma, USA*

The flexural and compressive strength, Knoop hardness, microstructure, shrinkage, and phase transformations of naturally occurring pyrophyllite and steatite were studied as a function of firing temperature. Both materials were fired in hydrogen and air, over the temperature ranges of 950 to 1100°C and 1000 to 1150°C for the steatite and pyrophyllite, respectively.

After firing the pyrophyllite at 1025°C or higher in hydrogen and 1050°C or higher in air a distinct change was noted in the microstructure which corresponds with significant increases in the strength and hardness. A similar correlation was observed for steatite following firing.

The strength and hardness of the hydrogen-fired pyrophyllite was higher than its air-fired counterpart. The opposite result was observed in the steatite.

## 1. Introduction

The fabrication of most ceramic electrical insulating materials is based on relatively simple configurations, mass production, and large volumes. Frequently, small quantities of electrical insulating ceramic materials are required for machining into intricate shapes. Two naturally occurring materials, pyrophyllite and steatite, frequently satisfy such requirements. These minerals, which exist in massive form, can be readily machined and then hardened by firing. The electrical properties of these materials have been reported [1, 2]; however, data relating mechanical strength to firing temperature are vague [3, 4]. It is well established [5] that small changes in firing temperature can appreciably affect the mechanical strength of ceramics.

The present investigation was initiated to determine the firing response of pyrophyllite and steatite over the temperature ranges of 1000 to 1150°C, and 950 to 1100°C, respectively. The flexural and compressive strengths were the mechanical parameters chosen for study as well as the effect of firing on hardness, phase changes, shrinkage, and microstructure. The microstructure was further characterised by electron probe analysis.

## 2. Experimental Procedure

### 2.1. Materials

The starting materials were naturally occurring steatite and pyrophyllite.‡ Chemical analyses and mechanical properties are given in tables I and II.

Pre-cut 2 × 2 × 3 in. blocks of steatite were generally white, but contained faint striations with a different texture, and slight gradations in colour. Samples were grouped according to the colour of the striations; grey, brown, or white. No significant difference was observed in the chemical and X-ray diffraction analyses between the colour groups. X-ray diffraction showed the presence of talc and a trace of kaolinite.

The pyrophyllite was obtained as a single 12 in.

---

*This work was conducted under the partial sponsorship of funds made available through National Aeronautics and Space Administration grants NGR-37-003-026 and NGL-37-003-026.

†Development Engineer, Halliburton Services, Halliburton Company, Duncan, Oklahoma.

‡Obtained from the American Lava Corporation under the trade name of Lava. The steatite was Lava Grade 1136. The pyrophyllite was Grade A.

**TABLE I** Chemical analysis of unfired materials (wt.%)

| Component | Pyrophyllite | Steatite |
|---|---|---|
| $SiO_2$ | 60.95 | 63.36 |
| $Al_2O_3$ | 29.9 | — |
| MgO | 0.11 | 30.8 |
| $Fe_2O_3$ | 1.50 | 0.41 |
| CaO | 0.03 | 0.28 |
| $K_2O$ | 0.52 | — |
| $Na_2O$ | 0.22 | 0.04 |
| LOI* | 6.71 | 4.68 |

*Loss on ignition. The data given are the average loss of all the bulk specimens fired.

**TABLE II** Mechanical properties of unfired materials.

| | Pyrophyllite | Steatite |
|---|---|---|
| Compressive strength (psi) | 6900 | 1600 |
| Flexural strength (psi) | 1600 | 62 |
| Knoop hardness ($kg/mm^2$)* | 57 | 9.7 |

*100 g load.

cube, grey in colour. X-ray diffraction analysis showed pyrophyllite and a trace of kaolinite.

## 2.2. Firing Procedure

The specimens were fired either in air or hydrogen in an electric muffle furnace. Air-fired specimens were placed on an alumina tray and heated at a 180° C per h to the desired temperature, held for 45 min., and cooled at the same rate. Temperature was monitored by a thermocouple positioned adjacent to the specimen.

The hydrogen fired specimens were placed in a retort, which was continuously purged with dry hydrogen. Heating rate was the same as in the case of the air-fired specimens. Gas flow was maintained at 5.0 l per min throughout the firing sequence, but was discontinued on cooling below 250° C.

## 2.3. Mechanical Properties

### 2.3.1. Flexural strength

The specimens were surface ground to 0.500 by 0.500 by approximately 1.75 in. prior to firing. Flexural strength was determined by four point loading according to ASTM Designation C78 [6] at a loading rate of 125 psi per sec.

### 2.3.2. Compressive strength

Specimens were machined to 0.750 in. diameter cylinders, 1.500 in. long prior to firing. Very smooth surfaces were obtained which eliminated the necessity for further surface preparation after firing. The compressive strength was determined according to ASTM Designation C407 [7] at a loading rate of 400 psi per sec.

### 2.3.3. Microhardness

The specimens used were those polished for the microscopic examination. Knoop hardness [8] was determined using a 100 g load.

## 2.4. Microscopic Examination and Electron Microprobe Analysis

Broken flexural strength specimens were polished by grinding on successively finer silicon carbide abrasive papers, finishing with 600 grit. They were then rough polished using 6 $\mu$m diamond, the final polish being on 0.3 $\mu$m alumina. These specimens were used for both microscopic examination and electron probe analyses. Carbon was vacuum deposited on the microprobe specimens to prevent charging. Total electron image and appropriate elemental scans were obtained for each matrial before and after firing. Concentrations of aluminium, silicon, and iron were determined semi-quantitatively in the particles and matrix of pyrophyllite.

## 2.5. Shrinkage

A linear expansion or shrinkage factor was determined from dimensional changes in flexural and compressive specimens upon firing.

# 3. Results and Discussion

## 3.1. Mechanical Properties

### 3.1.1. Pyrophyllite

Results of mechanical strength tests are given in figs. 1, 2, and 3. Mechanical strength and hardness responded to firing in a similar manner. Maxima were observed in all the strength or hardness versus firing temperature plots. Hydrogen firing generally resulted in strength and hardness values higher than for specimens fired in air. The pyrophyllite was grey when fired in hydrogen

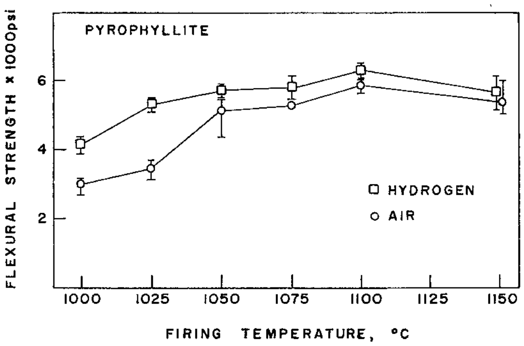

*Figure 1* Flexural strength versus firing temperature for pyrophyllite.

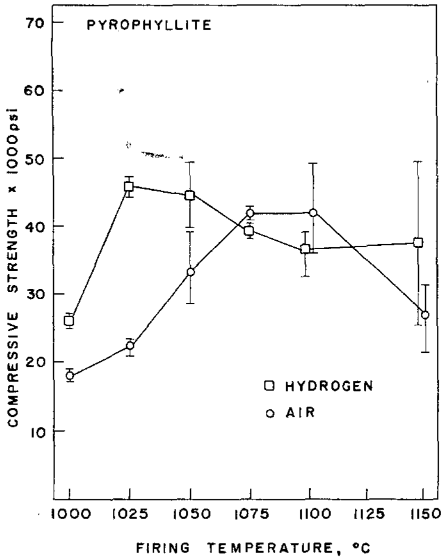

*Figure 2* Compressive strength versus firing temperature for pyrophyllite.

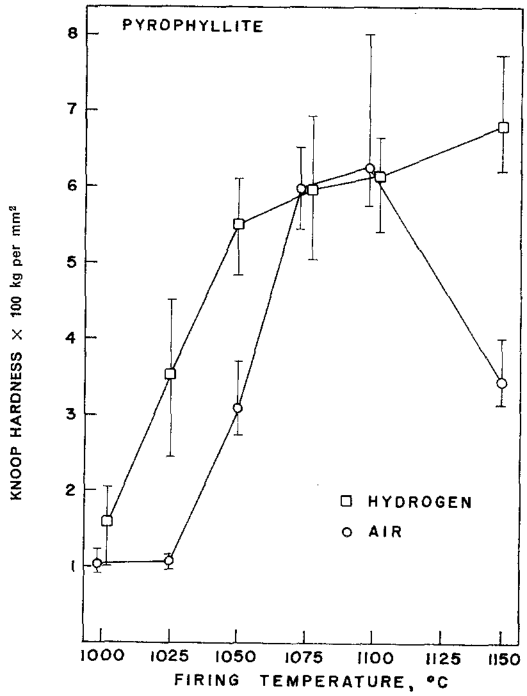

*Figure 3* Knoop hardness versus firing temperature for pyrophyllite.

but brown when fired in air. The difference in colour was probably due to the oxidation state of the iron impurity which may have also contributed to the observed difference in mechanical strength with firing atmosphere.

### 3.1.2. *Steatite*

Results of mechanical strength tests are given in figs. 4, 5, and 6. A maxima was again observed in all the strength and hardness versus firing temperature plots. Generally, air-fired steatite had a higher flexural strength and Knoop hardness than its hydrogen-fired counterpart. As with pyrophyllite, this may have been due to the oxidation state of the iron. The air and hydrogen-fired steatite samples were brown and white respectively.

Compressive strength was generally higher in samples fired in hydrogen than in air. This was probably due to internal cracks, naturally occurring flaws, observed in the steatite specimens (particularly the compressive specimens) after

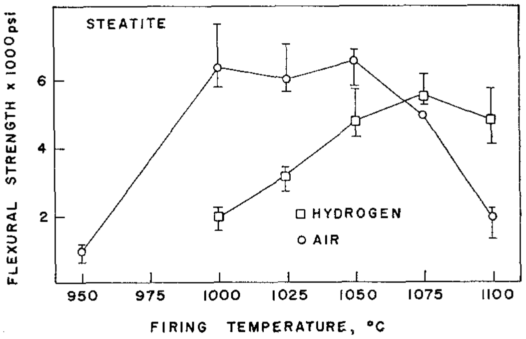

*Figure 4* Flexural strength versus firing temperature for steatite.

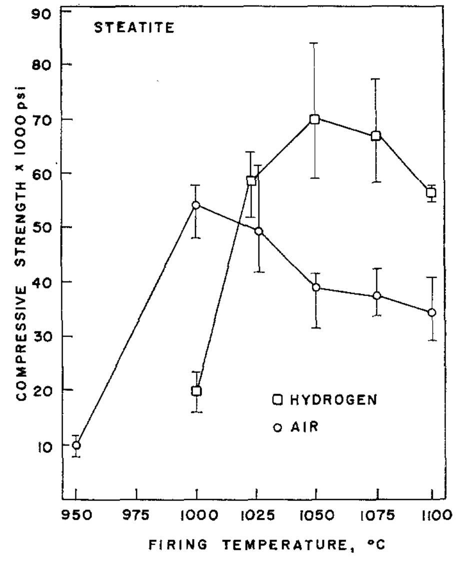

*Figure 5* Compressive strength versus firing temperature for steatite.

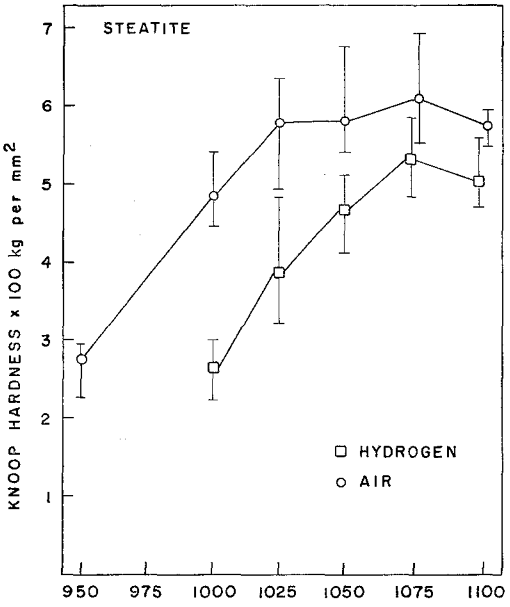

*Figure 6* Knoop hardness versus firing temperature for steatite.

firing. If cracking was visible the specimens were discarded, however, it is probable that subsurface cracks were not observed prior to testing. Compressive strength data at firing temperatures above 1025°C were probably unreliable due to the presence of cracks.

## 3.2. Microscopic Examination and Electron Probe Analysis

The microstructure of the pyrophyllite, before and after firing, consisted of two distinctly shaped particles (platelets and agglomerate particles) imbedded in a continuous matrix. The platelets and agglomerate particles in unfired and 1025°C hydrogen-fired pyrophyllite are marked A and B, respectively in fig. 7.

After firing at or above 1025°C in hydrogen or 1050°C or above in air, all platelets and particles dissolved into a single phase matrix. Above these temperatures, a transformation of pyrophyllite to mullite was indicated by X-ray diffraction analysis. The phase transformation and homogenisation of the matrix corresponds to the significant increases in the mechanical properties observed in figs. 1, 2 and 3.

The platelets (A in fig. 7a) became thicker and darker in colour after firing (A in fig. 7b) while the shape and colour of the agglomerate particles (B in fig. 7) remained unchanged. Semiquantitative electron probe analysis indicated that the chemical composition of the particles and the matrix did not change significantly with firing. The platelets, A in fig. 8, were higher in iron but lower in silicon and aluminium than the matrix. Electron probe data also indicated that the alumina to silica ratio of the platelets and the matrix was essentially the same. The platelets appear to be regions which are chemically similar to the matrix but which contain a higher concentration of iron.

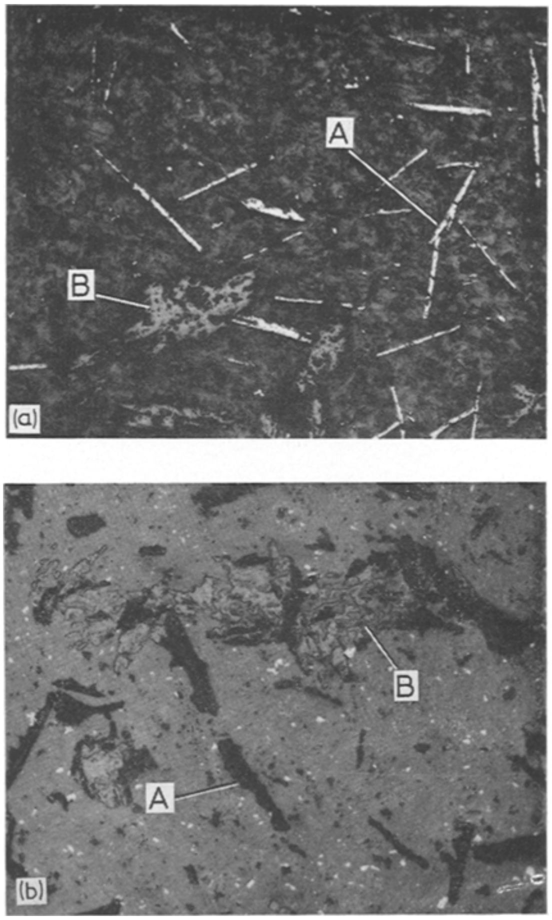

*Figure 7* Microstructure of pyrophyllite (a) unfired and (b) fired at 1025°C in hydrogen (× 200).

The agglomerate particles, B in fig. 8, appear to be an aluminium silicate low in iron but higher in aluminium and lower in silicon than the matrix. A higher concentration of iron was observed at the particle-matrix interface.

The microstructure of the steatite is shown in

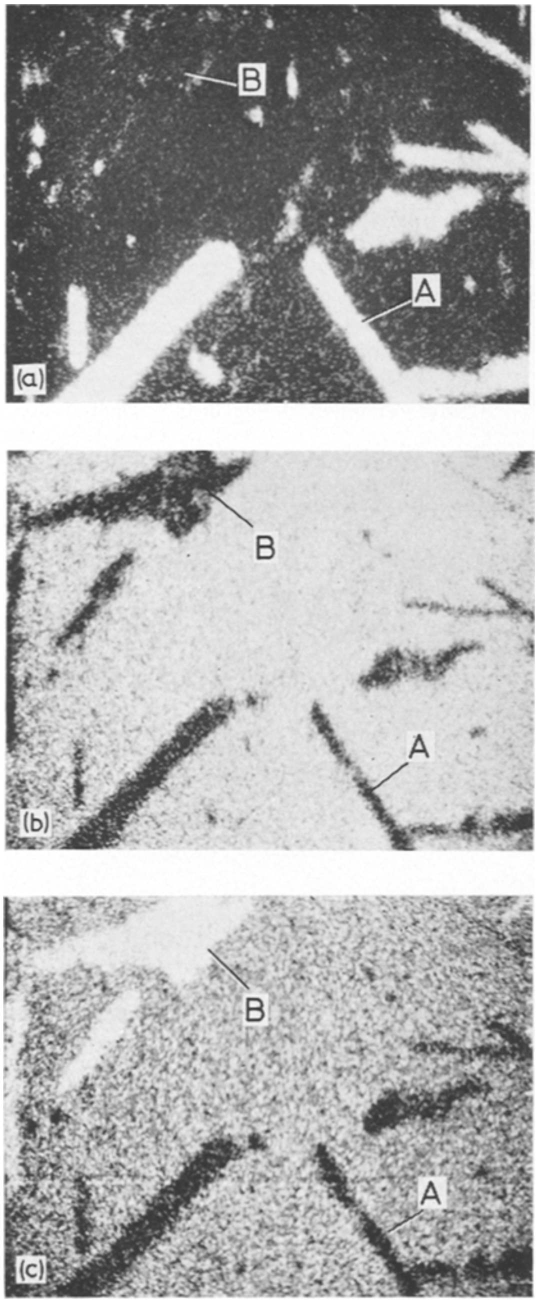

*Figure 8* Electron probe scans of unfired pyrophyllite (a) iron $K_\alpha$, (b) silicon $K_\alpha$, (c) aluminium $K_\alpha$ (× 500).

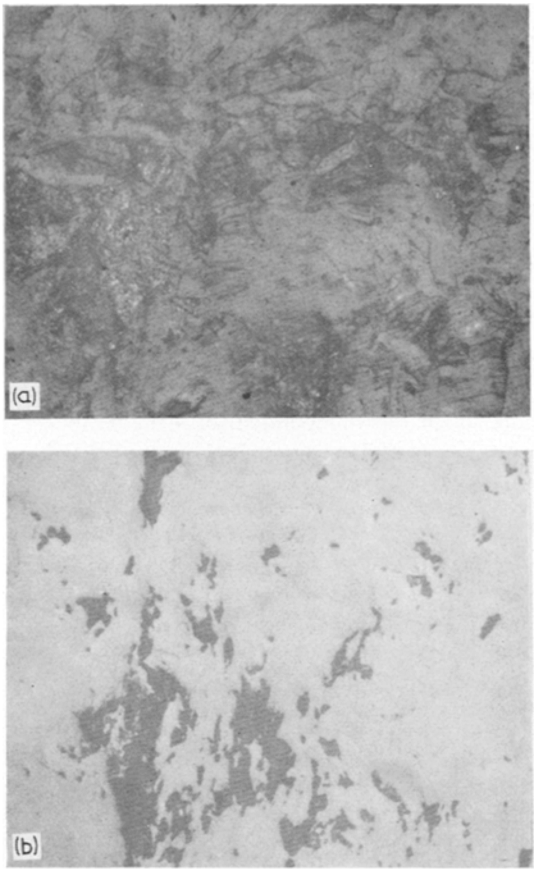

*Figure 9* Microstructure of steatite (a) unfired and (b) fired at 1075°C in hydrogen (× 200).

fig. 9. Dark particles in the fired material may be flaws just under, or intersecting the surface. After firing at or above 1000°C in air or 1025°C or above in hydrogen a single phase structure was observed along with a transformation of the steatite to ensteatite. The phase transformation corresponded well with significant increases in the mechanical properties observed in fig. 4, 5, and 6.

The electron probe analysis indicated that the magnesium and silicon were uniformly distributed throughout the material before and after firing.

### 3.3. Shrinkage

Shrinkage of either material did not vary significantly with firing temperature or atmosphere, except for the steatite fired at 950°C. The shrinkage in this case was 0.6% compared to 1.1% for the steatite fired at 1000°C or above. This low value was attributable, from weight loss measurements, to the incomplete removal of the water of hydration at 950°C.

The pyrophyllite expanded an average of 1.7% when fired.

## 4. Summary

The mechanical properties, phase transformations, and microstructure of naturally occurring pyrophyllite and steatite were studied as a function of firing temperature and atmosphere. With both materials a maximum value was observed in all mechanical properties. Mechanical strength was found to be a function of firing atmosphere and changes in strength and microstructure are related to phase transformations occurring at or above certain temperatures. Elemental distribution was determined before and after firing by electron probe analysis. A shrinkage factor was determined for both materials which was independent of firing temperature with the exception of steatite fired at 950°C.

## References

1. H. THURNAUER, *Electronics*, **12** (1939) 33.
2. F. ROSEBURY, "Handbook of Electron Tube and Vacuum Techniques" (Addison-Wesley, Reading, Massachusetts, 1965) p. 341.
3. J. EAGLE, *Amer. Ceram. Soc. Bull.* **26** (1947) 272.
4. H. INSLEY and V. FRECHETTE, "Microscopy of Ceramics and Cements" (Academic Press, London, 1955) p. 76.
5. I. IDA, Y. ARIA, M. FUKUDA, M. SUZUKI, K. INAMORI, M. SUGIURA, and H. TOKUNAGA, *Rev. Electrical Commun. Lab.* **15** Numbers 9-10 (1967) 623. Japan.
6. 1968 ASTM Book of Standards, Part 10, pp. 40-42, American Society for Testing and Materials, Philadelphia, Pennsylvania.
7. *Idem*, Part 13, pp. 345-47, American Society for Testing and Materials, Philadelphia, Pennsylvania.
8. F. KNOOP, C. PETERS, and W. EMERSON, *J. Res. Nat. Bur. Stand.*, **23** (1939) 34.

Received 14 September and accepted 29 October 1971.